Supplementary Materials and Methods

Expression and purification

The human 12-LOX wild type (wt) and mutants with the N-terminal 6xHistidine tag, were cloned into a pGen2 vector. 1L of Expi293 cells grown in Expi293 expression media were transiently transfected using Polyethylenimine (PEI) "Max" (1mg of DNA and 3 ml of 1mg/ml PEI) and the expression was carried out in a shaking incubator for 5 days at 37°C, 7% CO2. For the wt 12-LOX protein used for cryo-EM analysis the expression was performed in the presence of 1 μM ML355. The cell pellet was thawed and resuspended in lysis buffer (20 mM HEPES pH 8.0, 30 mM NaCl, 0.5 mM TCEP, 1 mM MgCl2, 500 units benzonase, 0.2 mM PMSF, 5 µg/ml leupeptin, 5 µg/ml soybean trypsin inhibitor) before being lysed by Dounce homogeniser using a tight pestle. Cell debris was removed by centrifugation (30,000 x g, 20 min, 4 °C) and the soluble portion was batch bound to Ni affinity resin for 1 hour at 4 °C. Ni affinity resin was packed into a glass column and washed with 10 column volumes of low salt wash buffer (20 mM HEPES pH 8.0, 150 mM NaCl, 0.5 mM TCEP, 10 mM imidazole) followed by 10 column volumes of high salt wash buffer (20 mM HEPES pH 8.0, 300 mM NaCl, 0.5 mM TCEP, 10 mM imidazole) before elution (20 mM HEPES pH 8.0, 150 mM NaCl, 0.5 mM TCEP, 500 mM imidazole). Eluted protein was concentrated in an Amicon Ultra-15 50 KDa molecular mass cut-off centrifugal filter unit (Millipore, Burlington, MA, USA) and further purified by SEC on a Superdex 200 Increase 10/300 GL (Cytiva, Marlborough, MA, USA) in SEC buffer (20 mM HEPES pH 8.0, 150 mM NaCl, 0.5 mM TCEP). Fractions were assessed for purity by SDS-PAGE, and fractions corresponding to tetramer or dimer were pooled separately. For the wt 12-LOX protein used in cryo-EM studies all purification buffers also contained 2-5 µM ML355. Protein was snap frozen in liquid nitrogen and stored at -80 °C.

Grid preparation and cryo-EM imaging

Samples were thawed, diluted to 1 mg/ml, and incubated at 4 °C with an additional 40 µM ML355. UltrAufoil R1.2/1.3 300 mesh holey grids (Quantifoil GmbH, Großlöbichau, Germany) were glow discharged in air at 15 mA for 180 s using a Pelco EasyGlow. 3 µl of sample was applied to the grids at 4 °C and 100% humidity and plunge frozen in liquid ethane using a Vitrobot Mark IV (Thermo Fisher Scientific, USA) with a blot time of 3s and blot force of -3. Data were collected on a G1 Titan Krios microscope (Thermo Fisher Scientific, USA) equipped with S-FEG, a BioQuantum energy filter and K3 detector (Gatan, Pleasanton, California, USA). The Krios was operated at an accelerating voltage of 300 kV with a 50 µm C2 aperture, 100 µm objective aperture inserted, and zero-loss filtering with a slit width of 10 eV, at an indicated magnification of 105kX in nanoprobe EFTEM mode. Data were collected using aberration-free image shift (AFIS) with Thermo Fisher EPU software. Further parameters for each dataset can be found in **Table S1.**

Tetramer cryo-EM image processing and model building

6896 movies collected at 0.82 Å/pix were motion corrected using UCSF MotionCor2 [1], and CTF parameters were estimated using GCTF[2]. 3.7 M particles were picked using autopicking within

RELION v3.1[3,4], and extracted particles were subject to multiple rounds of 2D and 3D classification with RELION v3.1. A set of particles (0.8 M) underwent 3D refinement, Bayesian polishing and CTF refinement before importing into cryoSPARC [5] where the last round of 2D classification and 3D heterogeneous refinement resulted in a final set of particles (0.5 M). The final set of particles underwent non-uniform 3D refinement with D2 symmetry, resulting in a 1.82 Å resolution map of the tetramer (FSC = 0.143, gold standard). Due to the high degree of flexibility between monomers, particles were subject to D2 symmetry expansion, and local refinement was performed on a monomer in cryoSPARC, which resulted in a 1.72 Å map. To model into the monomeric map, an initial predicted model was obtained from the AlphaFold Protein Structure Database[6,7], rigid body fit into the density using UCSF ChimeraX[8] and subject to repeated rounds of manual model building in COOT[9] and real-space refinement in PHENIX[10]. The refined monomer model was used to model into the tetramer map similarly. Lastly, the models were quality assessed using MolProbity[11] before PDB deposition.

3D variability analysis of tetramer

3D variability analysis (3DVA)[12] was performed using cryoSPARC using the final symmetry expanded particles (1.8 M). 3DVA was initially performed masked on the entire tetramer with 3 principal components output to 20 frames and analysed in UCSF ChimeraX[8]. 3DVA was further performed masked on a monomer with 3 principal components output in clustered mode (5 clusters). A subset of particles (0.3 M) with clear density in the ligand binding site was subject to local refinements yielding a monomer map at 1.90 Å and a tetramer map at 2.05 Å. These maps were used to model oleoyl-CoA into the ligand binding site. Modelling was performed as above, oleoyl-CoA was obtained from the monomer library (3 letter code – 3VV), and geometry restraints were generated using the GRADE webserver[13].

Dimer cryo-EM image processing and model building

4812 movies at 0.82 Å/pix were motion corrected using UCSF MotionCor2[1], and CTF parameters were estimated using GCTF[2]. 2.7 M particles were picked using Gautomatch using 2D projections of a previously processed 12-LOX dimer as a reference and extracted within RELION v3.1[3,4] with 4x downsampling (80-pixel box size at 3.28 Å/pix). Particles were imported into cryoSPARC[5] and subjected to 2D classification upon which the heterogeneity of the dataset became apparent. The 2D classes for the monomer, dimer, tetramer and the hexamer were manually selected and subjected to ab-initio reconstruction to create the starting models for each individual oligomeric state. The ab-initio models and an additional “junk” map were used for heterogeneous refinement of the entire dataset. From here on, the resulting particles for each oligomeric state were processed separately using similar strategies. First, each particle set was cleaned up using 2D classification. Then particle coordinates were imported back into Relion using pyem[14] for re-extraction at full resolution (320-pixel box at 0.82 Å/pix). Each particle set was then subjected to 2D classification, heterogenous and non-uniform refinement in cryoSPARC followed by CTF refinement and Bayesian polishing in Relion v3.1 followed by final round of non-uniform refinement in cryoSPARC. Specific processing details for each of the oligomeric states are stated below. The 12-LOX monomer particle set contained 35,994 particles and yielded a 2.76 Å resolution map (FSC = 0.143) after a non-uniform 3D refinement. The 12-LOX dimer particle set contained 126,914 particles and yielded a 2.53 Å (FSC = 0.143) resolution map following a non-

uniform 3D refinement. Each subunit of the dimer was further subjected to local refinement and 3D variability analysis to identify the least flexible classes. This yielded a “closed” (2.54 Å from 34,436 particles) and an “open” (2.33 Å from 126,914 particles) subunit conformations. The 12-LOX tetramer particle set contained 70,330 particles and yielded a 2.32 Å resolution map (FSC = 0.143) after a non-uniform 3D refinement in D2 symmetry. The local refinement of individual subunits following the symmetry expansion yielded a 2.1 Å map. The 12-LOX hexamer particle set contained 35,839 particles and yielded a 2.63 Å resolution map (FSC = 0.143) after a non-uniform 3D refinement in D3 symmetry. The local refinement of individual subunits following the symmetry expansion yielded a 2.24 Å map.

For modelling purposes of the 12-LOX dimer and the hexamer we created “composite” maps using Phenix suite[10]. To do this, for the 12-LOX dimer we combined the locally refined “open” and “closed” maps. For the 12-LOX hexamer we employed the locally refined single subunit map that was expanded using D3 symmetry. For modelling, the high-resolution model of the tetramer subunit (derived from the modelling into the highest resolution 1.72Å map of the tetramer) was rigid-body fit into the density maps of individual subunits of other oligomeric states using UCSF ChimeraX[8] and subject to repeated rounds of manual model building in COOT[9] and real-space refinement in PHENIX[10]. The ML355 and arachidonic acid (AA) were identified and manually built into 12-LOX. ML355 was generated from SMILES code, and geometry restraints were generated using the GRADE webserver[13]. AA was obtained from the monomer library (3 letter code – ACD). Lastly, the models were quality assessed using MolProbity[11] before PDB deposition.

Steady-State Kinetics

12-LOX reactions were performed at 22 °C in a 1 cm quartz cuvette containing 2 mL of 25 mM HEPES (pH 8.0) with AA varying from 0.25 to 25 μM. AA concentrations were determined by measuring the amount of oxylipins produced from complete reaction with soybean lipoxygenase-1 (SLO-1). Concentrations of 12-HpETE were determined by measuring the absorbance at 234 nm. Reactions were initiated by the addition ~20 μg of dimer 12-LOX and ~30 μg of tetramer 12-LOX and were monitored on a Perkin-Elmer Lambda 45 UV/Vis spectrophotometer. Product formation was determined by the increase in absorbance at 234 nm for 12-HpETE (ε_{234nm} = 25,000 M^{-1} cm^{-1}). KaleidaGraph (Synergy) was used to fit initial rates (at less than 20% turnover), to the Michaelis-Menten equation for the calculation of kinetic parameters.

To measure steady-state kinetics at 12-LOX WT and L589A, 5 nM of 12-LOX was incubated at 25 °C in 250 μL of 25 mM HEPES (pH 8.0), 150mM NaCl, 0.01% Triton-X, 0.5 μM tris(2-carboxyethyl)phosphine (TCEP) with AA varying from 6 to 1 μM in a 96w UV-STAR Microplate (Greiner Bio-One). AA concentrations were determined by measuring the absorbance at 257, 268 and 315 nm Concentrations of 12-HpETE were determined by measuring the absorbance at 234 nm in triplicate. Reactions were initiated by the addition of 12-LOX and were monitored on a BMG Labtech CLARIOstar plus plate reader. Product formation was determined by the increase in absorbance at 234 nm for 12-HpETE (ε234nm = 25,000 M−1 cm−1) every five seconds for 90 seconds total. Graphpad Prism was used to fit initial rates to the Michaelis-Menten equation for the calculation of kinetic parameters.

IC_{50} Determination

The IC_{50} values for the 12-LOX specific inhibitor, ML355, against dimer 12-LOX and tetramer 12-LOX were determined in the same manner as the steady-state kinetic values. The reactions were carried out in 25 mM HEPES buffer (pH 8.0), 0.01% Triton X-100, and 10 μM AA. IC_{50} values were obtained by determining the enzymatic rate at nine inhibitor concentrations and plotting rate against their inhibitor concentration, followed by a hyperbolic saturation curve fit. The data used for the saturation curve fits were performed in duplicate or triplicate, depending on the quality of the data. Triton X-100 was used to ensure proper solubilization of the fatty acid and inhibitor. The acyl-CoAs were purchased from Avanti Polar Lipids. The IC_{50} values for the acyl-CoAs against dimer 12-LOX SEC peak were determined in a similar manner as described above.

To measure ML355 inhibition at L589A, IC_{50} values for ML355 were determined in a similar manner as steady state kinetic values for L589A. 3 to 0.003 μM ML355 were inhibited with 5 nM 12-LOX WT or L589A for 10 minutes at RT before initiation of the reaction through addition of 2 μM AA in triplicate. Product formation was determined by the increase in absorbance at 234 nm for 12-HpETE (ε_{234nm} = 25,000 M^{-1} cm^{-1}) at 25 °C every five seconds for 90 seconds total using a BMG Labtech CLARIOstar plus. Graphpad Prism was used to calculate initial rate against their inhibitor concentration, followed by a one-site inhibition fit.

Synthetic Liposome Preparation and 12-LOX Binding

A lipid suspension was prepared from commercial sources with the following molar ratios: 99.9:0.1 DOPC: DSPE-PEG (i.e. DOPC). Each lipid mixture was dissolved in chloroform and the solutions were left under N_2 for 20 min and placed in a vacuum chamber for at least 12 h at room temperature to remove all traces of solvent. Lipid mixtures were dissolved in 25 mM HEPES buffer (pH 8) to a concentration of 10 mg/mL and incubated in glass vials on a tube rotator for 1 h to facilitate homogenization. Liposomes were created using the literature protocol[15] using a 100 nm filter. Liposome suspension volumes were adjusted to have a final concentration of 10 mg/mL and their size were determined by dynamic light scattering (DLS).

Liposome suspensions were placed on a DynaMag™-2 for 15 min at room temperature to bind the liposomes. Supernatant was removed and 1 mL of 25 mM HEPES buffer (pH 8) was added. This washing step was repeated five times, after which time 30 μg of dimer or tetramer were added to 1 mL of a 10 mg/mL liposome suspension. The sample was rocked over ice for 10 min and then placed on a DynaMag™-2 for 10 min. 25 μL of the supernatant was saved, and the beads were resuspended to a final volume of 1 mL. 25 μL of the resuspended beads were saved and both saved samples were subjected to SDS-PAGE and subsequent Western analysis. The antibodies were isolated from rabbit sera subjected to 12-LOX exposure (Pocono Rabbit Farm). Using ImageLab, ratios of the supernatant to pellet were determined. All conditions were done in triplicate.

Mass photometry analysis of 12-LOX oligomeric populations.

Combined SEC fractions from the “dimer” and the “tetramer” peaks from 12-LOX purification were analysed using mass photometry. The protein was diluted to 100 nM in 20 mM Hepes pH 7.5,

150 mM NaCl. The measurements were performed using a TwoMP mass photometer (Refeyn) and analysed using the corresponding software (DiscoverMP). First, we performed an autofocus stabilisation using 10 μl of the buffer. Following this, we added the 10 μl of the diluted 12-LOX fractions and reordered a 60 s movie. The calibration curve was created using BSA (128 kDa), catalase (240 kDa) apoferritin (440 kDa) and thyroglobulin (660 kDa).

Assessment of protein stability by thermal unfolding

SEC fractions from the "dimer" and "tetramer" peaks of 12-LOX mutant purifications were diluted to 0.5 mg/ml in 20 mM Hepes pH 7.5, 150 mM NaCl, 0.5 mM TCEP. Each 10 µl sample, transferred into a capillary, was heated from 35 to 95 °C using a Tycho NT.6 (Nanotemper). The unfolding of 12-LOX was tracked via changes in intrinsic tryptophan fluorescence at 330 and 350 nm. The 350/330 nm fluorescence ratio was plotted and the melting temperature (Tm) (inflection point) compared between wt12-LOX and the mutants. The data was analysed using the software included with the instrument.

References

1. Zheng SQ, Palovcak E, Armache J-P, Verba KA, Cheng Y, Agard DA. MotionCor2: anisotropic correction of beam-induced motion for improved cryo-electron microscopy. *Cell Research*. 2017;14(4):331-332.
2. Zhang K. Gctf: Real-time CTF determination and correction. *Journal of Structural Biology*. 2016;193(1):1-12.
3. Zivanov J, Nakane T, Forsberg BO, et al. New tools for automated high-resolution cryo-EM structure determination in RELION-3. *Elife*. 2018;7:163.
4. Scheres SHW. A Bayesian View on Cryo-EM Structure Determination. *Journal of molecular biology*. 2012;415(2):406-418.
5. Punjani A, Rubinstein JL, Fleet DJ, Brubaker MA. cryoSPARC: algorithms for rapid unsupervised cryo-EM structure determination. *Nat Methods*. 2017;14(3):290-296.
6. Varadi M, Anyango S, Deshpande M, et al. AlphaFold Protein Structure Database: massively expanding the structural coverage of protein-sequence space with high-accuracy models. *Nucleic Acids Res*. 2022;50(D1):D439-D444.
7. Jumper J, Evans R, Pritzel A, et al. Highly accurate protein structure prediction with AlphaFold. *Nature*. 2021;596(7873):583-589.
8. Pettersen EF, Goddard TD, Huang CC, et al. UCSF ChimeraX: Structure visualization for researchers, educators, and developers. *Protein Sci*. 2021;30(1):70-82.
9. Emsley P, Lohkamp B, Scott WG, Cowtan K. Features and development of Coot. *Acta Crystallographica Section D*. 2010;66(Pt 4):486-501.
10. Adams PD, Afonine PV, Bunkóczi G, et al. PHENIX: a comprehensive Python-based system for macromolecular structure solution. *Acta Crystallographica Section D*. 2010;66(Pt 2):213-221.
11. Chen VB, Arendall WB, 3rd, Headd JJ, et al. MolProbity: all-atom structure validation for macromolecular crystallography. *Acta Crystallogr D Biol Crystallogr*. 2010;66(Pt 1):12-21.
12. Punjani A, Fleet DJ. 3D variability analysis: Resolving continuous flexibility and discrete heterogeneity from single particle cryo-EM. *J Struct Biol*. 2021;213(2):107702.
13. Smart OS, Womack TO, Sharff A, et al. grade v.1.2.13. *wwwglobalphasingcom*. 2011.
14. Asarnow D, Palovcak E, Cheng Y. UCSF pyem v0.5; 2019.

15. Voss OH, Lee HN, Tian L, Krzewski K, Coligan JE. Liposome Preparation for the Analysis of Lipid-Receptor Interaction and Efferocytosis. *Curr Protoc Immunol*. 2018;120:14 44 11-14 44 21.

Supplementary Figure 1

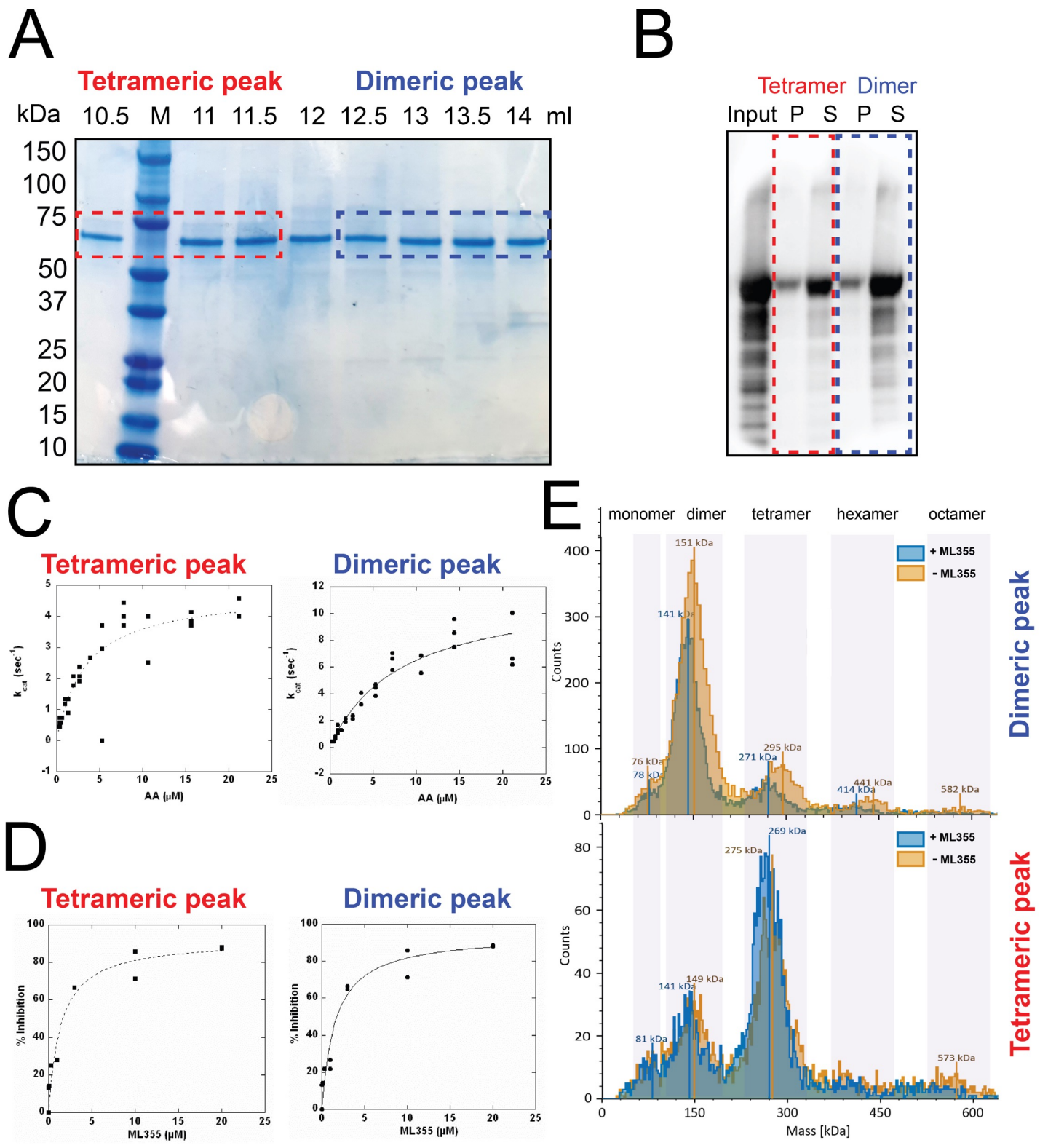

Supplementary Figure 1. Purification and characterization of 12S-Lipoxygenase (12-LOX). (A) SDS-PAGE of fractions following SEC of 12-LOX expressed and purified from HEK-293. (B) Liposome binding of 12-LOX "dimeric" and "tetrameric" peaks. Western Blot from a representative liposome binding experiment. P- pellet fraction; S-soluble fraction. (C-D) Enzymatic properties (C) and Inhibition (D) of 12-LOX "dimeric" and "tetrameric" peaks. (E) Size distributions within 12-LOX "dimeric" and "tetrameric" peaks assessed by mass photometry in the absence or presence of 25 μM ML355.

Supplementary Figure 2

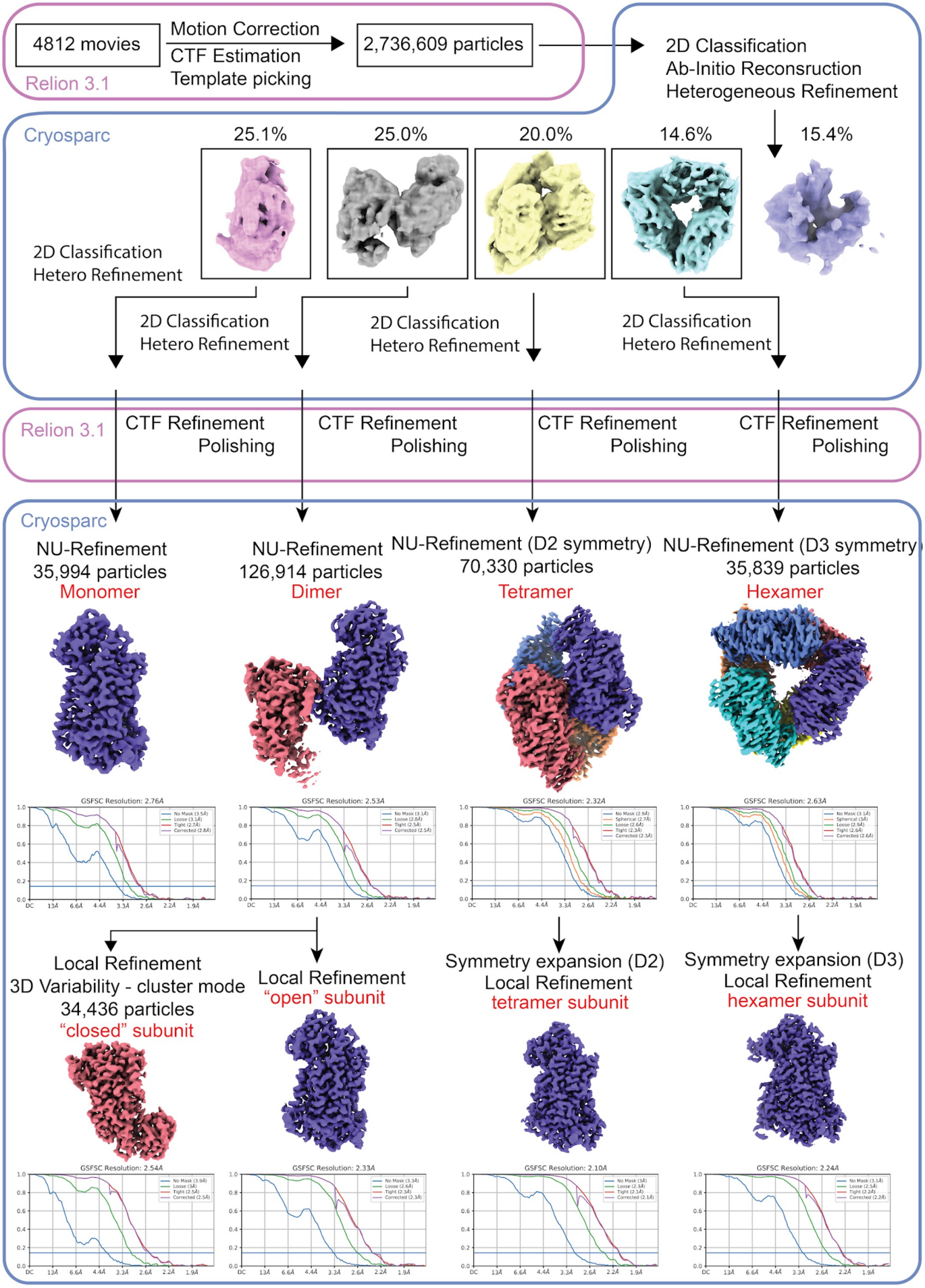

Supplementary Figure 2. Cryo-EM data processing for dimer 12-LOX. Workflow to achieve high-resolution structures of 12-LOX monomers, dimers, tetramers and hexamers from the "dimeric" SEC peak from 12-LOX purification .

Supplementary Figure 3

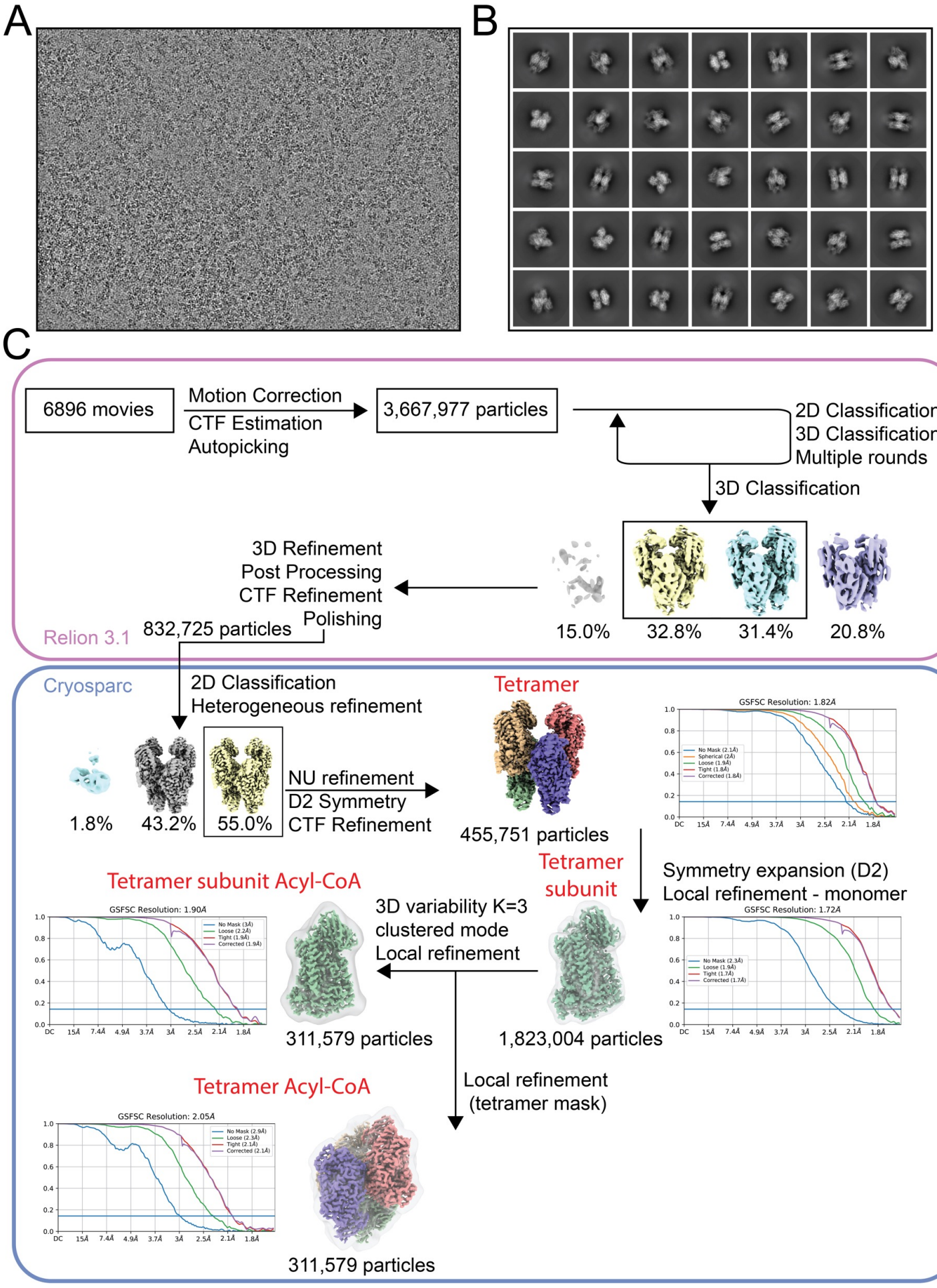

Supplementary Figure 3. Cryo-EM data processing for tetramer 12-LOX. (A) Representative micrograph and (B) representative 2D classifications. (C) Workflow to achieve high-resolution structures of 12-LOX tetramers from the "tetrameric" SEC peak from 12-LOX purification .

Supplementary Figure 4

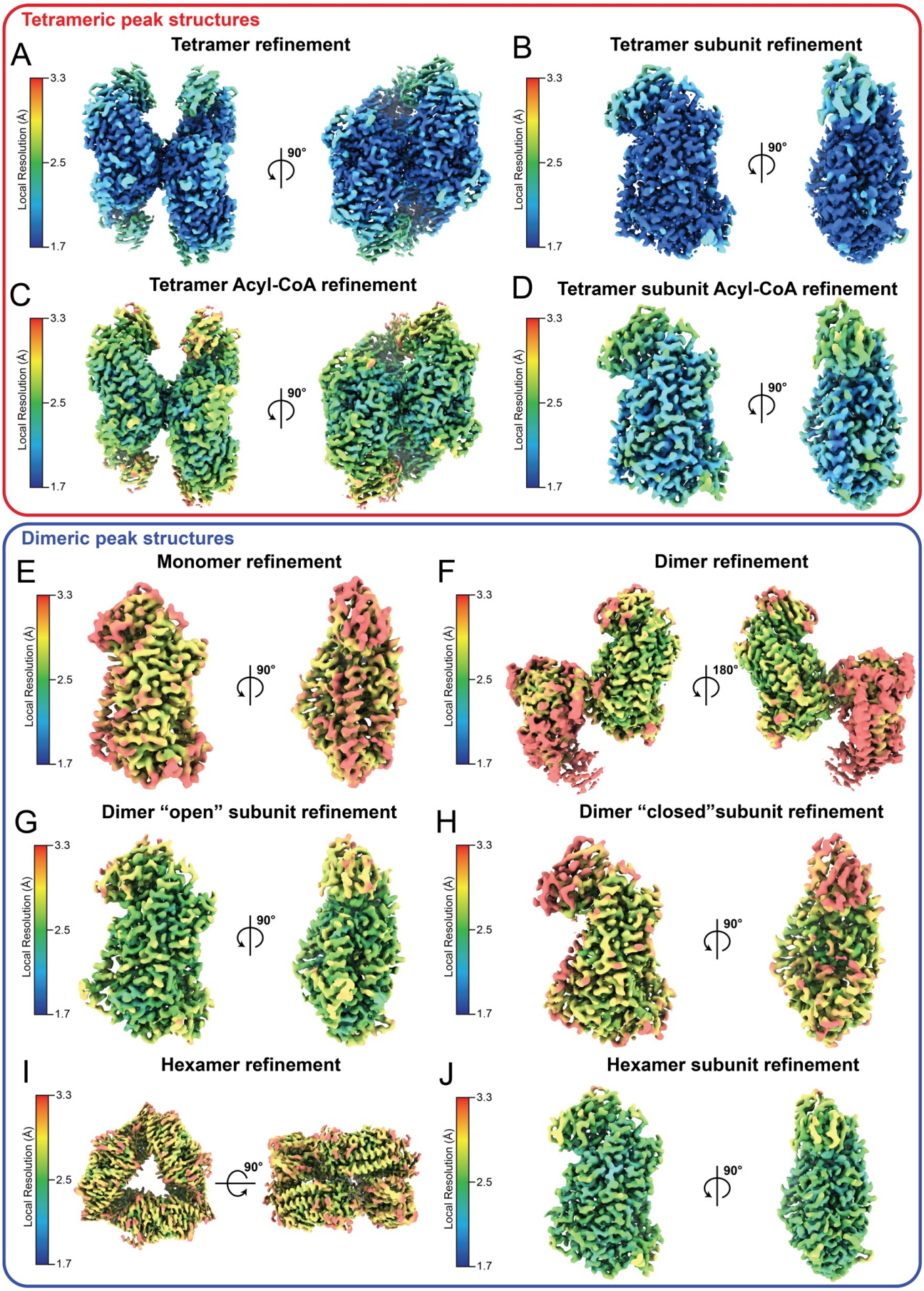

Supplementary Figure 4. Cryo-EM density maps coloured by local resolution. (A) Highest-resolution map of 12-LOX tetramer from the "tetrameric" SEC peak and corresponding monomer after local refinement (B). (C) The map of 12-LOX tetramer following the refinement to improve Acyl-CoA density and corresponding monomer after local refinement (D). (E) The map of 12-LOX monomer from the "dimeric" SEC peak. (F) The map of 12-LOX dimer from the "dimeric" SEC peak and corresponding "open" (G) and "closed" (H) subunits following local refinement. (I) The map of 12-LOX hexamer from the "dimeric" SEC peak and corresponding monomer after local refinement (J).

Supplementary Figure 5

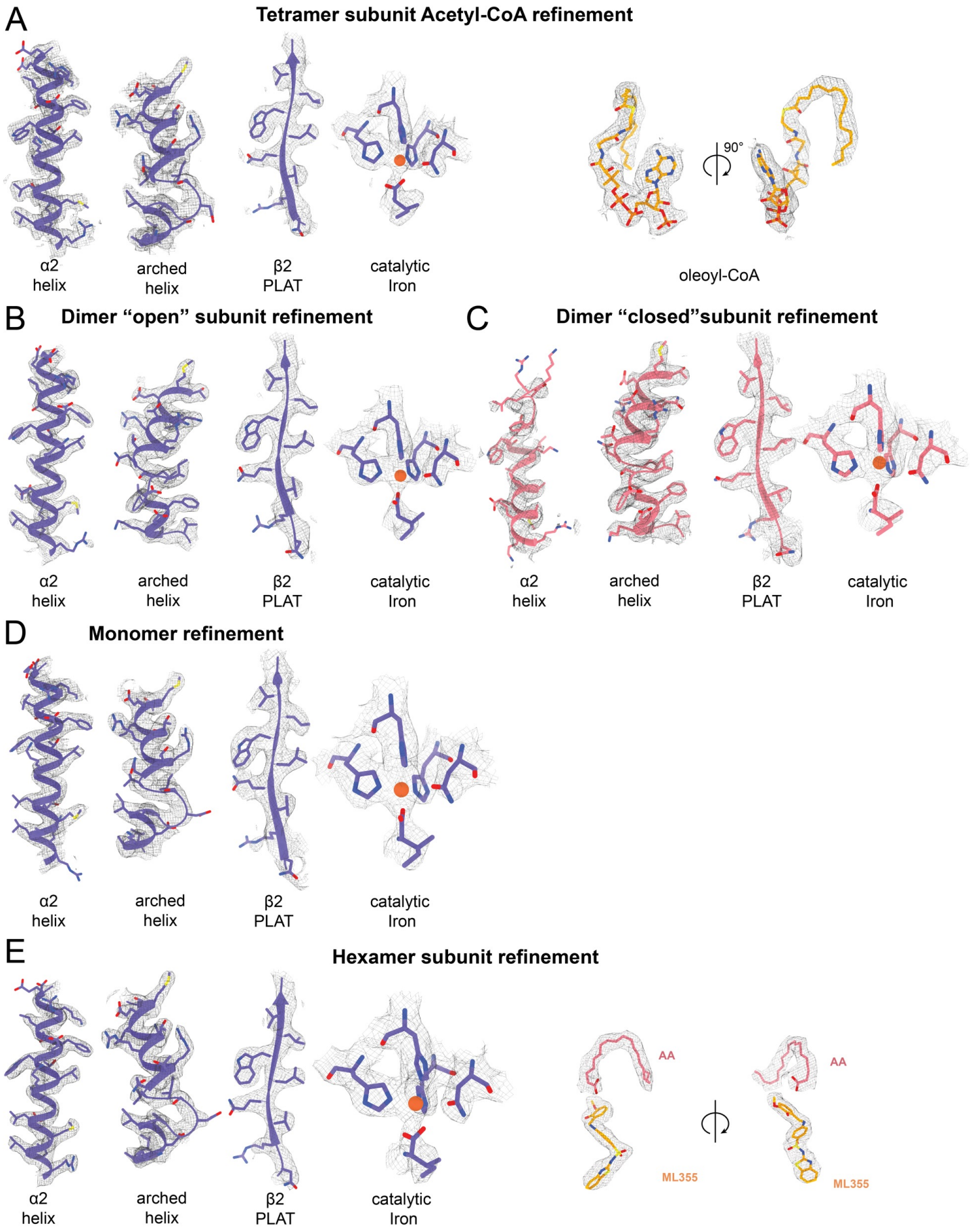

Supplementary Figure 5. Representative regions of the cryo-EM maps . (A) The map of 12-LOX tetramer from the "tetrameric" SEC peak following the refinement to improve Acyl-CoA density. (B-C) The maps of "open" (B) and "closed" (C) subunits of 12-LOX dimer from the "dimeric" SEC peak after local refinement. (D) The map of 12-LOX monomer from the "dimeric" SEC peak. (E) The map of 12-LOX hexamer from the "dimeric" SEC peak after local refinement. The molecular model is shown in sticks and the cryo-EM map in mesh

Supplementary Figure 6

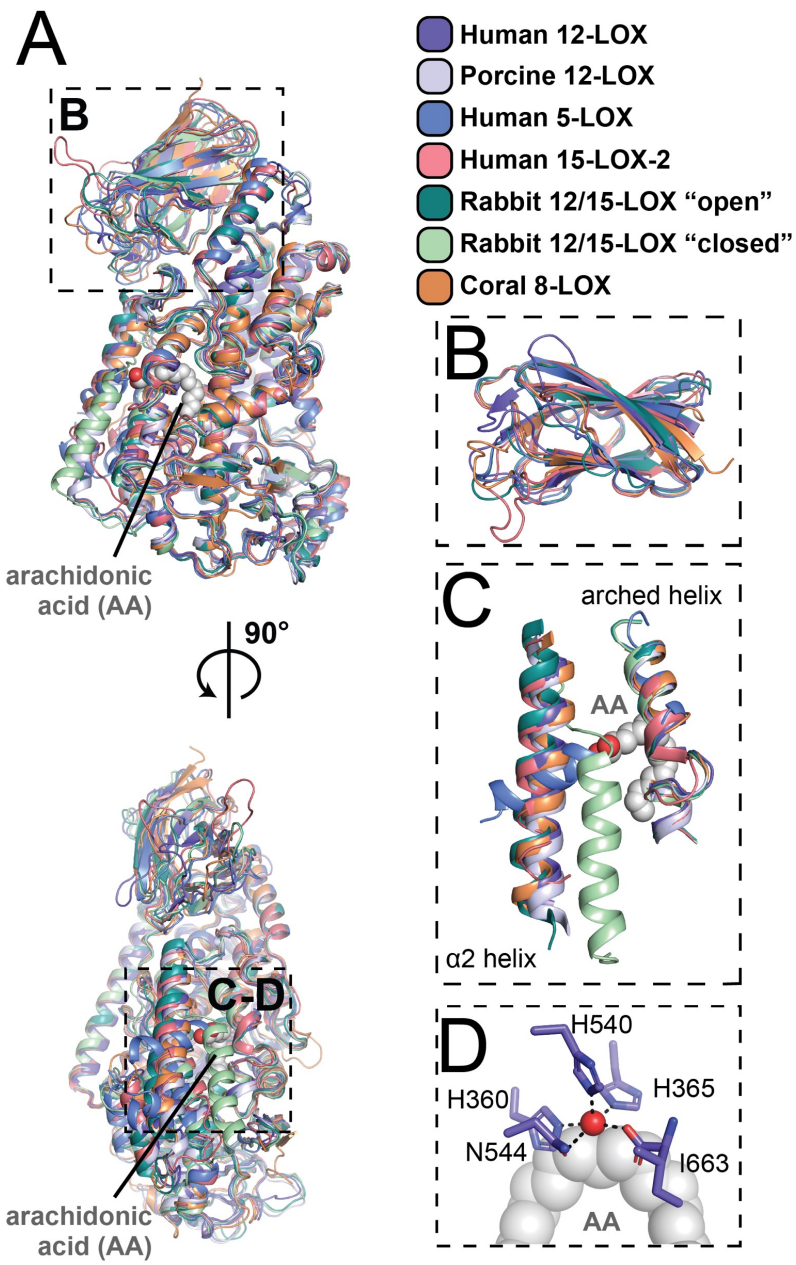

Supplementary Figure 6. Comparison of the 12-LOX and other LOXs. Comparison of cryo-EM structure of human 12-LOX to porcine 12-LOX (PDB: 3RDE), human 5-LOX (PDB: 3V99), human 15-LOX-2 (PDB: 4NRE), 12/15-LOX in "open" and "closed" states (PDB: 2P0M) and arachidonic acid (AA) bound Coral 8-LOX (PDB: 4QWT). (A) Overall comparison. (B) PLAT-domain comparison. (C) Arched helix and α2-helix comparison. (D) Catalytic Iron site of 12-LOX with AA displayed from Coral 8-LOX. Fe atom is shown as a red sphere. FE-coordinating residues are shown in sticks.

Supplementary Figure 7

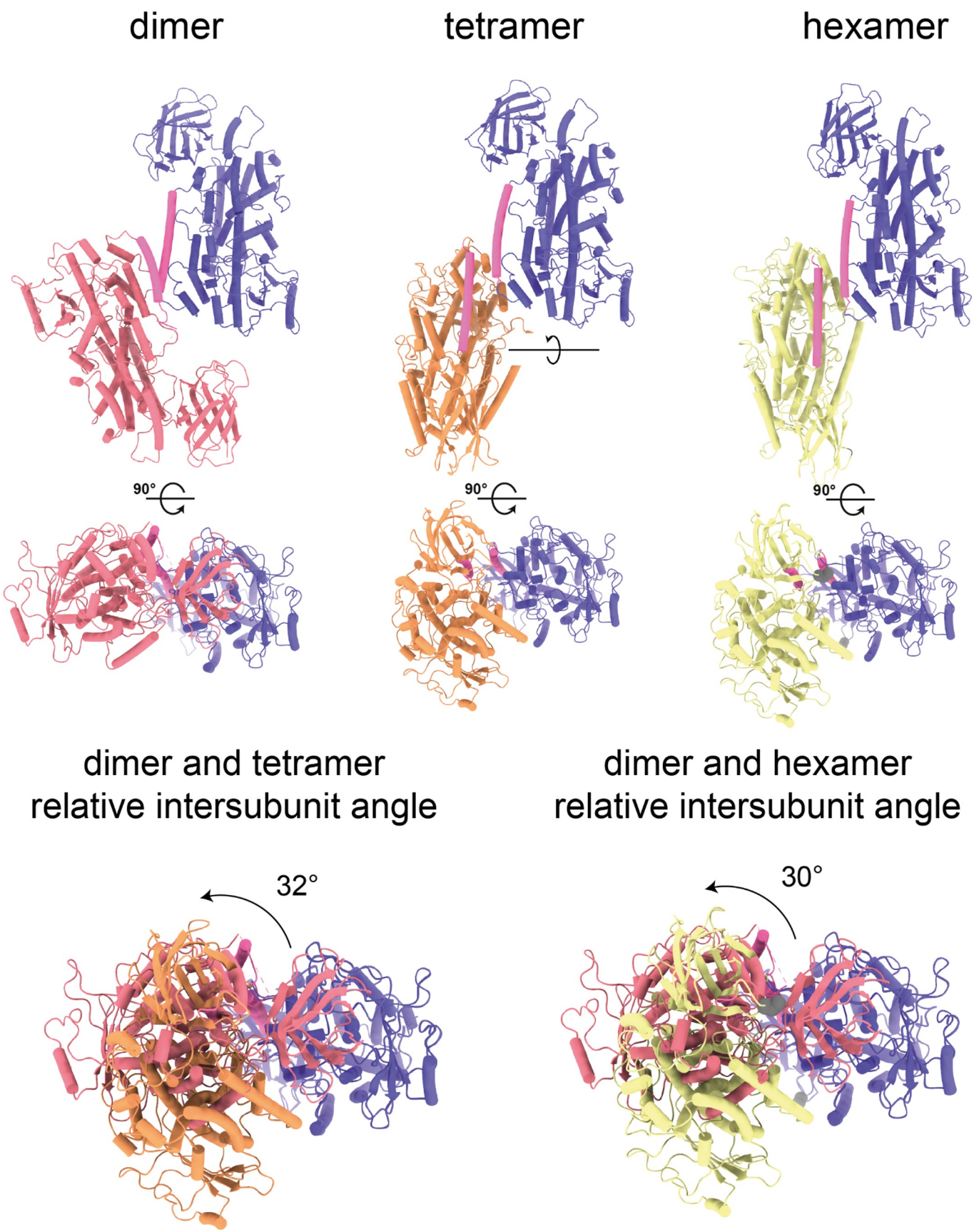

Supplementary Figure 7. Dimers as biological units of 12-LOX. 12-LOX exists as a dimer, dimer of dimers (tetramer), and trimer of dimers (hexamer). (Top) Dimer arrangement of each oligomeric form. (Bottom) Alignment of dimeric 12-LOX to the dimers with tetramer (left) and hexamer (right) showing the relative chain rotation within the dimers.

Supplementary Figure 8

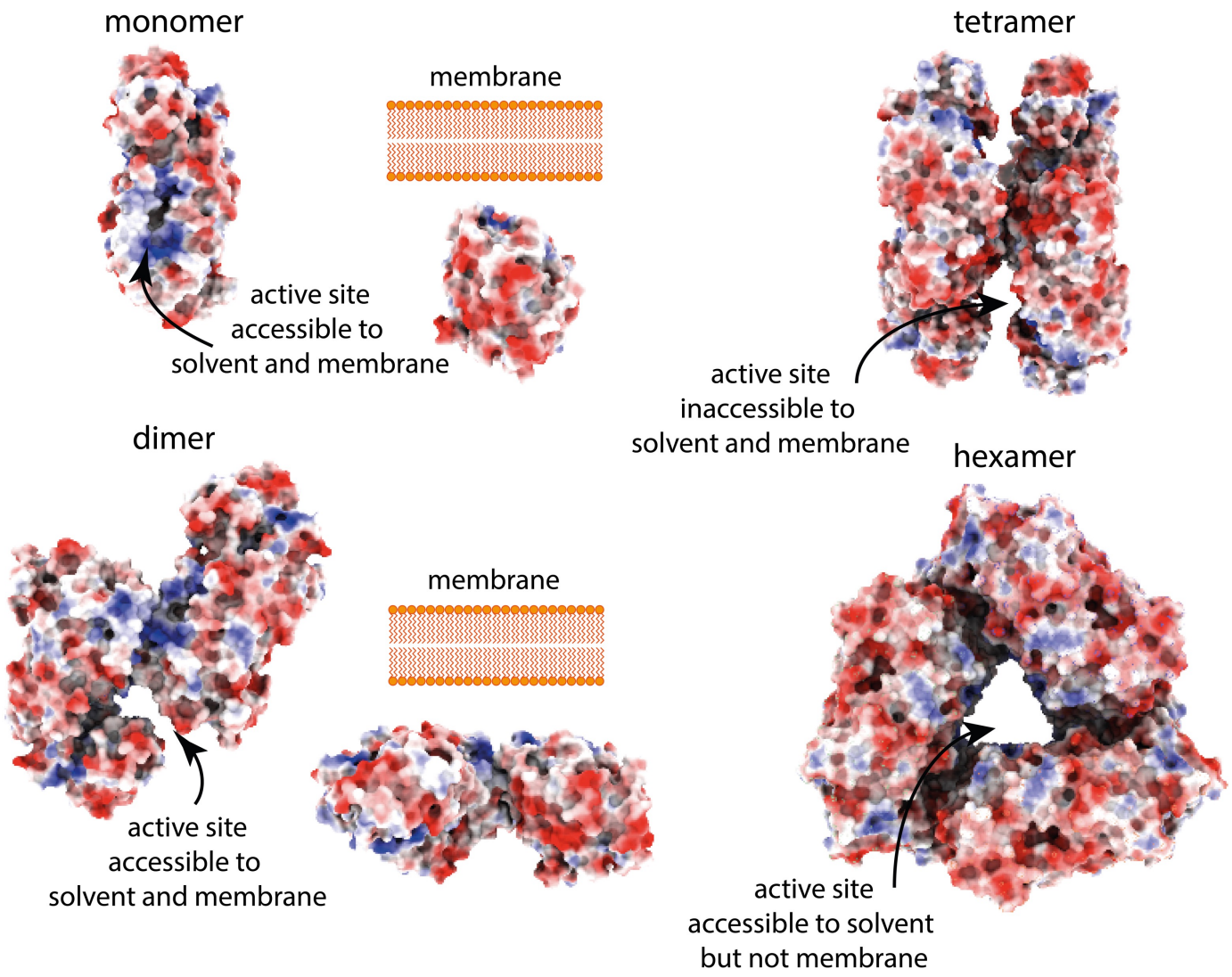

Supplementary Figure 8. Proposed mechanism of membrane association for 12-LOX oligomers. 12-LOX displayed as surface and coloured according to surface electrostatic potential (red is negative, white neutral and blue positive). The predicted membrane-binding surface is exposed and is available for membrane binding in 12-LOX monomers and dimers but is occluded in tetramers and hexamers.

Supplementary Figure 9

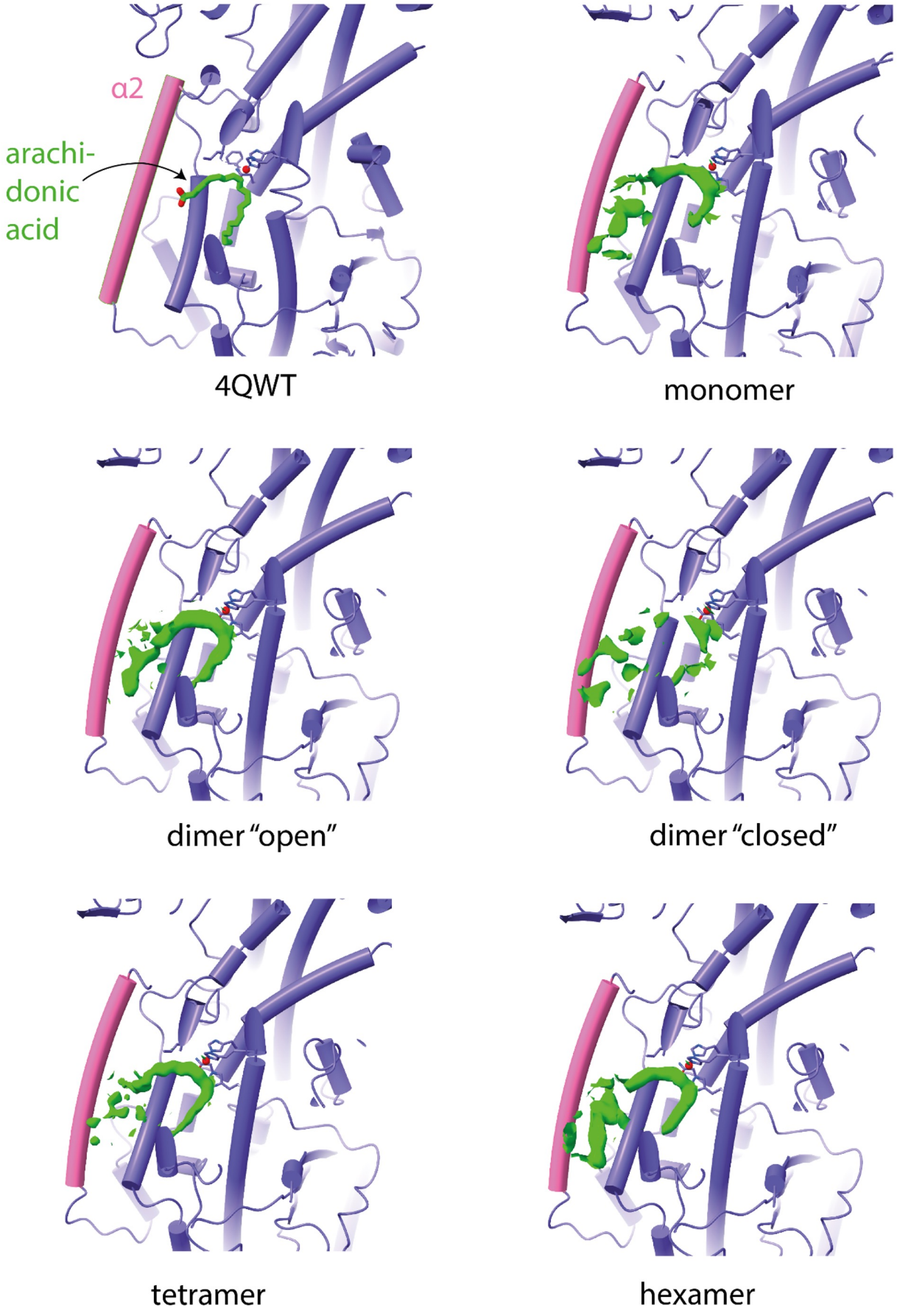

Supplementary Figure 9. Small molecule density within the active site of 12-LOX. In all 12-LOX subunits in the "open" conformation the active site is occupied by continuous density. 12-LOX catalytic domain is shown in purple cylindrical cartoons, the α2-helix is in pink. The density within the active site of each oligomeric form is shown as a green volume. Fe atom is shown as a red sphere.

Supplementary Figure 10

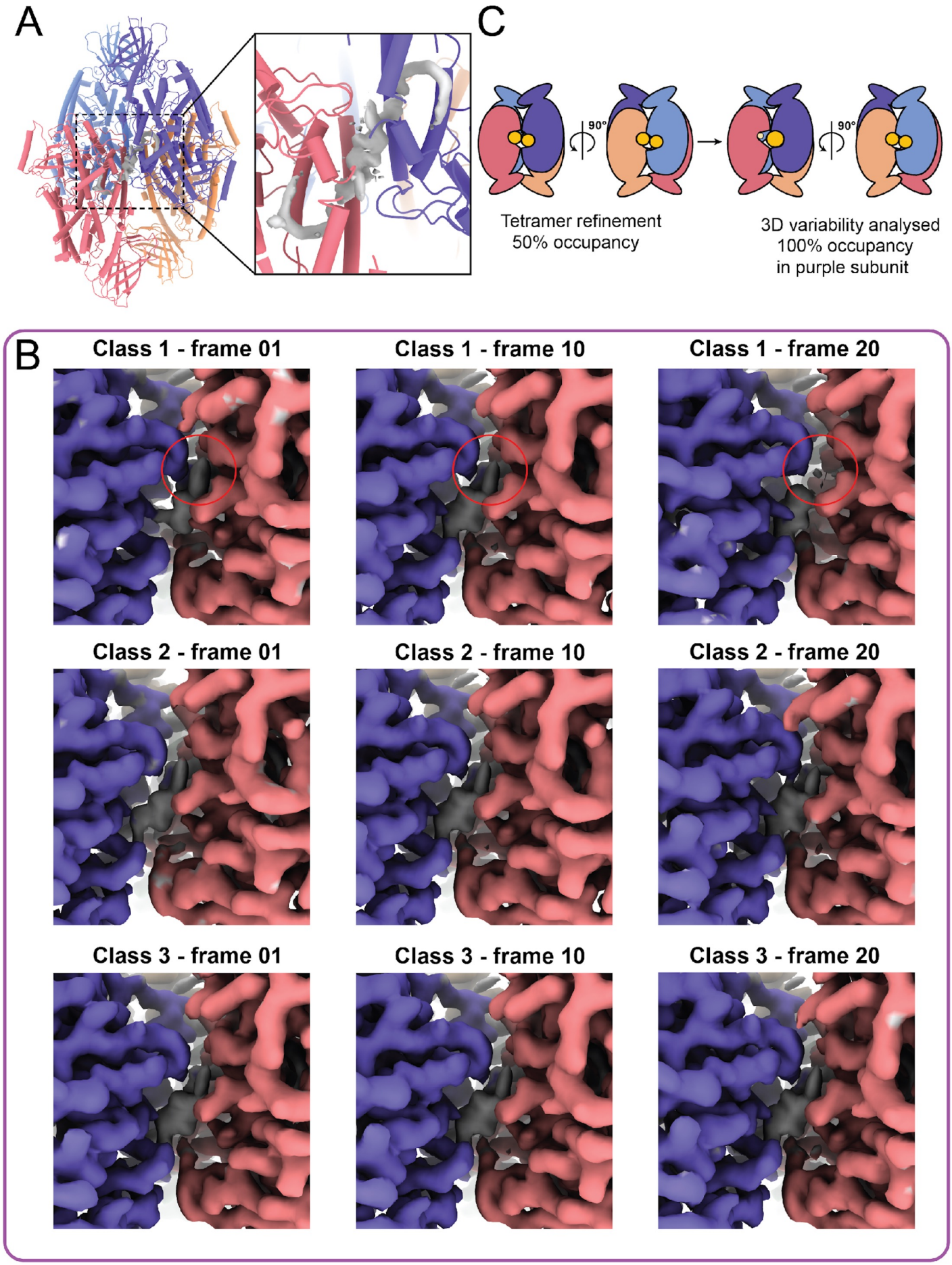

Supplementary Figure 10. 3D-variability of the tetrameric 12-LOX showing the acyl-CoA occupancy in the active site. (A) Model of 12-LOX tetramer with density in the catalytic site shown as grey volume. (B) 3D-variability analysis of 12-LOX tetramer. 12-LOX subunits are displayed as coloured volume (red and purple) and the catalytic site as grey volume. The red circle denotes changes observed in catalytic site density. (C) Graphical representation of ligand density.

Supplementary Figure 11

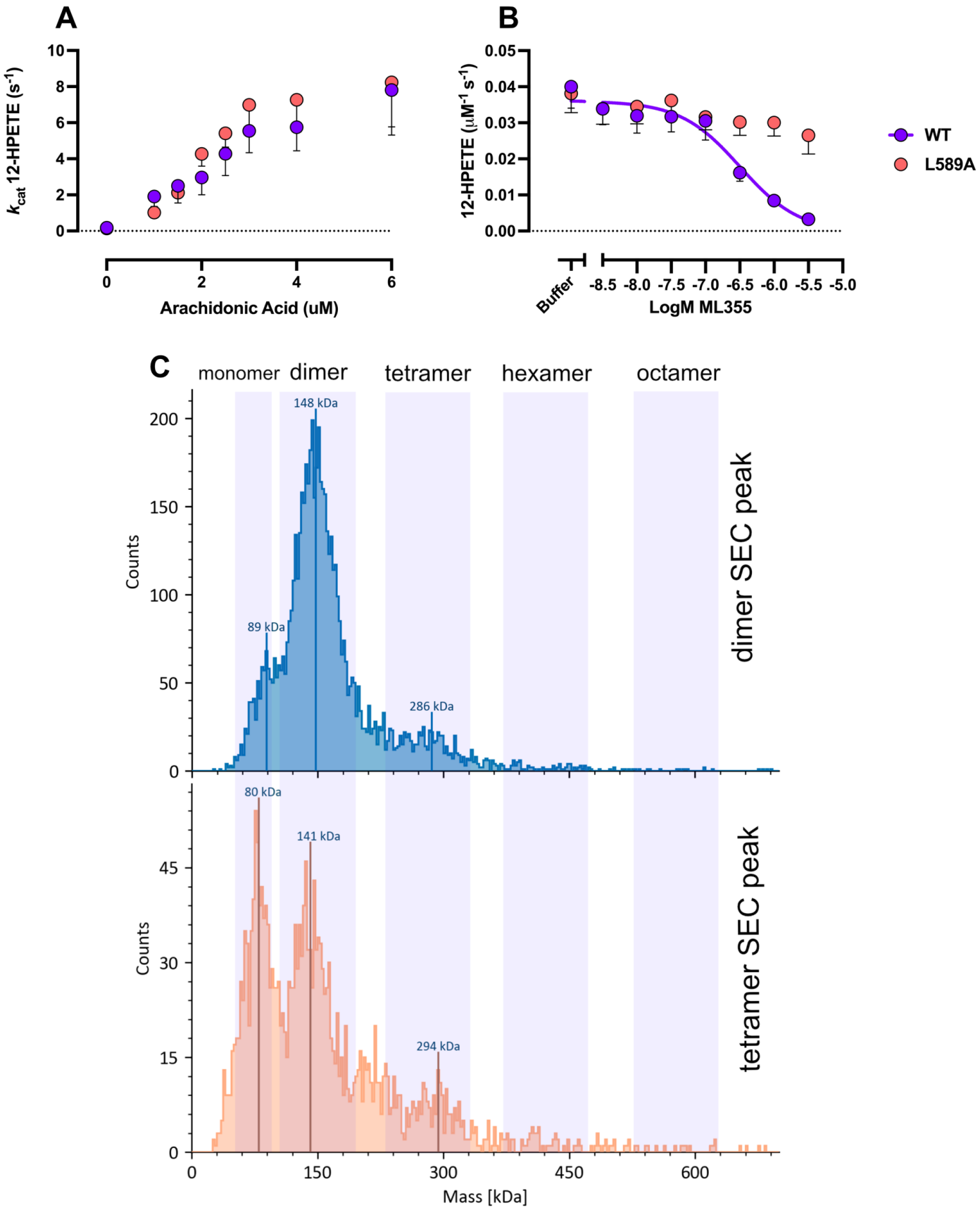

Supplementary Figure 11. Characterisation of the L589A 12-LOX mutant. (A-B) Enzymatic properties (A) and Inhibition (B) of the L589A 12-LOX. (C) Size distributions within L589A 12-LOX "dimeric" and "tetrameric" peaks assessed by mass photometry.

Table S1. Cryo-EM data collection, refinement, and validation statistics

	12-LOX Monomer	12-LOX Dimer	12-LOX Hexamer	12-LOX Tetramer
Data Collection	Dimer SEC peak			Tetramer SEC peak
EMD code	EMD-40039	EMD-40040	EMD-40041	EMD-40042
PDB code	8GHB	8GHC	8GHD	8GHE
Micrographs	4182			6896
Electron Dose (e^-/A^2)	60			60
Voltage (kV)	300			300
Pixel size (Å)	0.82			0.82
Spot Size	5			5
Exposure time	4.8			4.8
Movie frames	60			60
K3 CDS mode	yes			yes
Defocus range (μm)	0.5-1.5			0.5-1.5
Refinement				
Symmetry imposed	C1	C1	Consensus* D3 1 subunit C1	C1 (due to the asymmetry of ligand binding)
Particles (final map)	35,994	Consensus* 126,914 "open" 126,914 "closed" 34,436	Consensus* 35,839 1 subunit 215,034	Tetramer*** 311,579 "Oleoyl-CoA" 311,579 "Consensus"*455,751 "1 subunit" 455,751
Resolution @0.143 FSC (Å)	2.76	Consensus* 2.53 "open" 2.33 "closed" 2.54	Consensus* 2.63 1 subunit 2.24	Tetramer***2.05 "Oleoyl-CoA"1.90 "Consensus"*1.82 "1 subunit"1.72
$CC_{map-model}$	0.85	Composite** 0.79	Composite** 0.89	Tetramer***0.90
Map sharpening B factor ($Å^2$)	-30	Consensus* -60 "open" -25 "closed" -25	Consensus* -73 1 subunit -25	Tetramer***-43 "Oleoyl-CoA"-39 "Consensus"*-47 "1 subunit"-44
Model Quality		Refined against the composite** map	Refined against the composite** map	Refined against the tetramer*** map
R.M.S. deviations				
Bond length (Å)	0.006	0. 004	0.005	0.004
Bond angles (°)	0.821	0.793	0.820	0.663
Ramachandran				
Favoured (%)	97.25	97.77	98.16	98.45
Outliers (%)	2.75	2.23	1.84	1.55
Rotamer outliers (%)	0	0	0	0.04
C-beta deviations (%)	0	0	0	0
Clashscore	4.09	4.55	4.04	3.72
MolProbity score	1.33	1.28	1.19	1.16

* Consensus maps are maps prior to local refinement of individual subunits.

**For the 12-LOX dimers and hexamers we performed the final refinements against the composite maps generated in Phenix suite from local refinement maps. Dimer 12-LOX – we combined the local refinement maps for "open" and "closed" subunits. Hexamer 12-LOX – we applied the D3 symmetry to generate the entire hexamer from the locally refined single subunit.

***Tetramer 12-LOX – Following 3D variability classification of 1 subunit resulting in Oleoyl-CoA subunit map, focused refinement was performed to recover a Oleoyl-CoA bound tetramer map.

Table S2. Enzymatic properties and inhibition of two h12-LOX peaks from SEC. . The values are from at least 3 independent experiments. The standard deviation is shown in parenthesis.

	12-LOX dimer SEC peak	12-LOX tetramer SEC peak
Enzymatic activity		
Kcat (s^{-1})	11.8 (0.9)	4.8 (0.2)
Km (μM^{-1})	8.2 (1.0)	3.3 (0.7)
Kcat/Km (μM^{-1} s^{-1})	1.4 (0.01)	1.4 (0.01)
ML355 inhibition		
IC50 (μM)	1.6 (0.3)	1.4 (0.3)
Max inhibition (%)	95 (5)	92 (5)

Table S3. h12-LOX dimer SEC peak inhibition by acyl-CoAs. The values are from at least 3 independent experiments. The standard deviation is shown in parenthesis.

Substrate	IC50 (μM)
Palmitoyl-Coenzyme A (16:0)	> 200
Palmitoleoyl-Coenzyme A (16:1)	> 350
Stearoyl-Coenzyme A (18:0)	> 200
Oleoyl-Coenzyme A (18:1)	32 (4)
ɣ-Linolenoyl-Coenzyme A (18:3)	> 200
Arachidonoyl-Coenzyme A (20:4)	112 (20)